Experimental and Theoretical UV Characterizations of Acetylacetone and Its Isomers

S. Coussan,*,[†] **Y. Ferro,**[†] **A. Trivella,**[†] **M. Rajzmann,**[†] **P. Roubin,**[†] **R. Wieczorek,**[‡] **C. Manca,**[§]
P. Piecuch,[⊥,∥] **K. Kowalski,**[⊥] **M. Włoch,**[⊥] **S. A. Kucharski,**[⊥,#] **and M. Musiał**[#]

*Laboratoire Physique des Interactions Ioniques et Moléculaires, UMR 6633, Université de Provence-CNRS,
Centre St-Jérôme, 13397 Marseille Cedex 20, France, Faculty of Chemistry, University of Wroclaw, Joliot
Curie 14, 50−383 Wroclaw, Poland, Laboratorium für Physikalische Chemie, ETH Zürich, CH8093 Zürich
Switzerland, Department of Chemistry, Michigan State University, East Lansing MI 48824, Department of
Physics and Astronomy, Michigan State University, East Lansing, Michigan, and 48824, Institute of Chemistry,
University of Silesia, Szkolna 9, 40−006 Katowice, Poland*

Received: November 24, 2005; In Final Form: January 18, 2006

Cryogenic matrix isolation experiments have allowed the measurement of the UV absorption spectra of the
high-energy non-chelated isomers of acetylacetone, these isomers being produced by UV irradiation of the
stable chelated form. Their identification has been done by coupling selective UV-induced isomerization,
infrared spectroscopy, and harmonic vibrational frequency calculations using density functional theory. The
relative energies of the chelated and non-chelated forms of acetylacetone in the S_0 state have been obtained
using density functional theory and coupled-cluster methods. For each isomer of acetylacetone, we have
calculated the UV transition energies and dipole oscillator strengths using the excited-state coupled-cluster
methods, including EOMCCSD (equation-of-motion coupled-cluster method with singles and doubles) and
CR-EOMCCSD(T) (the completely renormalized EOMCC approach with singles, doubles, and non-iterative
triples). For dipole-allowed transition energies, there is a very good agreement between experiment and theory.
In particular, the CR-EOMCCSD(T) approach explains the blue shift in the electronic spectrum due to the
formation of the non-chelated species after the UV irradiation of the chelated form of acetylacetone. Both
experiment and CR-EOMCCSD(T) theory identify two among the seven non-chelated forms to be characterized
by red-shifted UV transitions relative to the remaining five non-chelated isomers.

I. Introduction

Systems with a strong intramolecular hydrogen bond have
given rise to numerous theoretical and experimental studies,
especially malonaldehyde[1−11] and acetylacetone.[4,12−30] Indeed,
these molecules are among the simplest molecules exhibiting a
H-bond along with a proton-tunneling exchange between the
oxygen atoms. Figure 1 illustrates the keto−enol equilibrium
of acetylacetone which is almost totally shifted toward the enol
form in gas phase[31] and when isolated in cryogenic matrices.
Figure 1 also shows the eight isomers of the enol forms labeled
XYZ, the three letters being either *C* or *T*, where *C* stands for
the cis character and *T* stands for the trans character relative to
the C−C, C=C, and C−O bonds, respectively; in this nomen-
clature, the chelated form, which is the most stable one, is
labeled CCC.

Previous theoretical studies have concentrated on pro-
ton[13,17,24,25] or hydrogen[5,6] transfer and on strength of the
H-bond,[16] whereas very few studies have been done on the UV
transitions and UV-induced reactivity. In a previous study, we
have shown[2,14] that broad band UV excitations of acetylacetone
and malonaldehyde isolated in cryogenic matrices lead to the
isomerization of the CCC stable form and to the observation of

the high-energy non-chelated forms. Conversely, in gas phase[26]
or in molecular beam,[20,21] dissociation occurs. We have also
recently photoisomerized acetylacetone trapped in a nitrogen
matrix using both laser UV and IR irradiation,[27] to emphasize
the selectivity and to discriminate from broad band irradiation.
This type of experiment has shown to be a very powerful tool
for identifying the different isomers. It should be noted that
trapping in cryogenic matrices has up to now been the only
way to observe and study these isomers.

We focus here on the characterization of the UV absorption
spectrum of the different isomers of acetylacetone isolated in a
nitrogen matrix using, in addition to the standard UV absorption
spectroscopy, UV-induced reactivity, infrared spectroscopy, and
vibrational frequency calculations. The complete set of relative
energies of the isomers of acetylacetone in the electronic ground
state (S_0) has also been calculated using coupled-cluster
methods, including the completely renormalized coupled-cluster
approach with singles, doubles, and non-iterative triples or CR-
CCSD(T), for short.[32−35] The UV transition energies and dipole
oscillator strengths, which are essential for the analysis of the
observed spectrum and spectral shifts, have been calculated at
the equation-of-motion coupled-cluster (EOMCC) level of
theory, including the recent extension of the ground-state CR-
CCSD(T) approach to excited states via the EOMCC formal-
ism.[33,35,36] The theoretical and experimental UV transition
energies are compared and analyzed.

II. Experimental Section

A. Method. Acetylacetone ($C_5H_8O_2$, > 99% purity, Aldrich-
Chemie) distilled under vacuum and nitrogen (N60 grade, Air

* Corresponding author: coussan@up.univ-mrs.fr.
† Laboratoire Physique des Interactions Ioniques et Moléculaires, UMR
6633, Université de Provence-CNRS.
‡ Faculty of Chemistry, University of Wroclaw.
§ Laboratorium für Physikalische Chemie, ETH Zürich.
⊥ Department of Chemistry, Michigan State University.
∥ Department of Physics and Astronomy, Michigan State University.
Institute of Chemistry, University of Silesia.

Acetylacetone and Its Isomers

J. Phys. Chem. A, Vol. 110, No. 11, 2006 **3921**
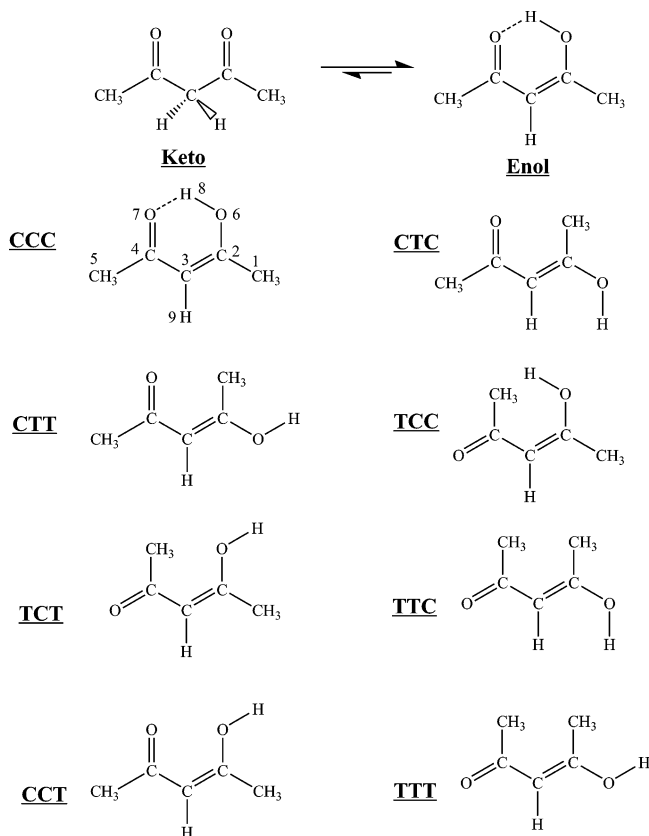
Figure 1. Keto−enol equilibrium; Schematic picture of the chelated (CCC) and seven non-chelated forms of the enol isomer. C stands for the cis character and T stands for the trans character relative to the C−C, C=C, and C−O bonds, respectively.

Figure 2. UV spectra of acetylacetone isolated in a N_2 matrix (concentration, 1/5000; temperature, 17 K). The different types of irradiation have been done successively in the order indicated in the legend.

TABLE 1: Harmonic Vibrational Frequencies (in cm^{-1}) of the ν_{OH}, $\nu_{C=O}$, and $\nu_{C=C}$ Modes and the $\Delta\nu = |\nu_{C=O} - \nu_{C=C}|$ Values for Acetylacetone and Its Isomers, Obtained at the B3LYP/6-311++G(2d,2p) Level of Theory

	ν_{OH}	$\nu_{C=O}$	$\nu_{C=C}$	$\Delta\nu$
CCC	3022.9	1643.3	1674.2	30.9
CTC	3797.4	1734.1	1635.6	98.5
CTT	3826.4	1738.7	1657.4	81.3
TCC	3808.6	1707.0	1667.0	40.0
TCT	3839.2	1704.0	1711.9	7.9
TTC	3801.6	1698.2	1671.2	27.0
CCT	3819.9	1751.0	1668.5	82.5
TTT	3836.0	1694.4	1703.4	9.0

Liquid) gas were mixed in a vacuum line using standard manometric techniques. For UV spectroscopy, roughly 0.5 Pa m^3 of a 1:5000 mixture was rapidly sprayed onto a CsI window maintained at 17 K inside a cryostat using a close-cycled helium cryogenerator (CTI-cryogenics). UV spectra were recorded by transmission through the window held at the deposition temperature with a SAFAS 190 DES spectrometer at a 2 nm resolution. No significant effect was observed when varying the temperature from 10 to 25 K. For IR spectroscopy, roughly 4 Pa m^3 of a 1:500 mixture was sprayed onto a Au-plated Cu cube maintained at 17 K and the sample was then maintained at 4 K, using a close-cycled helium cryogenerator (Cryomech-PT405). Infrared spectra (FTIR) were recorded with a IFS 66/S Bruker spectrometer in reflection-transmission mode, at a 0.12 cm^{-1} resolution. The IR measured frequencies were compared with the previously calculated harmonic vibrational frequencies,[27] obtained using the B3LYP/6-311++G(2d,2p) level of density functional theory, as implemented in GAUSSIAN 98.[37] The calculated harmonic vibrational frequencies and frequency shifts are summarized in Table 1.

UV irradiation were performed by doubling the signal coming from an optical parametric oscillator pumped by a Nd:YAG laser at 355 nm (VEGA, BM Industrie, Thalès), the pulse duration being about 6 ns, the repetition rate 10 Hz, and the resolution about 1 nm. For the sample, the average fluence was a few tenths of millijoules and the beam diameter was about 5 mm.

B. Results. Figure 2 shows the UV absorption spectra recorded for acetylacetone isolated in a nitrogen matrix, before and after various irradiation times. After deposition, a broad band centered at 265 nm is observed, corresponding to the stable chelated CCC form. Spectra taken after 15, 30, 45, and 60 min

of irradiation at 265 nm ($P \sim 10$ mW) are also plotted: the band progressively shifts toward 230 nm, no further effect being observed for longer irradiation times. The spectrum taken after a reverse 15 min irradiation at 230 nm indicates a reverse conversion to the initial CCC form, with no further changes after longer irradiation times. The absorption maximum found for chelated acetylacetone is in agreement with the 266 nm value obtained in the cases of molecular beam[20,21] and flow cell experiments.[26] The full width half-maximum (fwhm) of the bands centered at 265 and 230 nm is about 30 nm. We have previously shown that the 230 nm band corresponds to the formation of non-chelated forms,[27] these forms being clearly characterized using FTIR spectroscopy by the appearance of free ν_{OH} bands in the 3640−3560 cm^{-1} region. Note that low temperatures prevent back-reactions and allow for the observation of these high-energy isomers. Figure 2 shows that there is no isobestic point for the chelated ⇌ non-chelated conversion, which indicates that there are at least three types of species corresponding to three UV bands. We have fitted UV spectra and obtained a consistent fit with three bands of Gaussian shape, centered, respectively, at 265 ± 1, 249 ± 1, and 230 ± 1 nm, as shown in Figure 3. The corresponding fwhm values are 30, 29, and 27 nm, respectively.

We present here another series of experiments for which the UV excitation of acetylacetone has been carried out in a similar way, and for which the FTIR results are now analyzed. Figure 4a shows the infrared absorption spectrum recorded immediately after deposition, and Figure 4b shows the difference spectrum after 23 min of irradiation at 265 nm ($P \sim 8$ mW), in the stretching ν_{OH} and $\nu_{C=O}/\nu_{C=C}$ mode regions. New bands appear after the irradiation in the 3630−3570 cm^{-1} region, corresponding to free ν_{OH} modes of non-chelated isomers. To facilitate our analysis, we divide the free ν_{OH} bands into the following
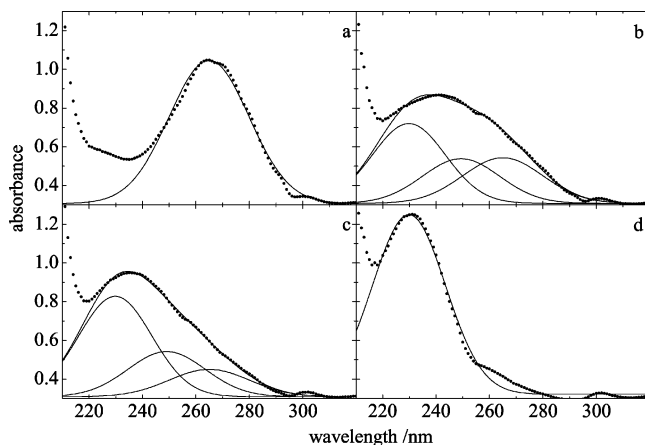
Figure 3. Fits of the UV spectra obtained for acetylacetone isolated in a N_2 matrix to bands of Gaussian shape: before irradiation (a) and after irradiation at 265 nm for 15 (b), 30 (c), and 60 min (d).
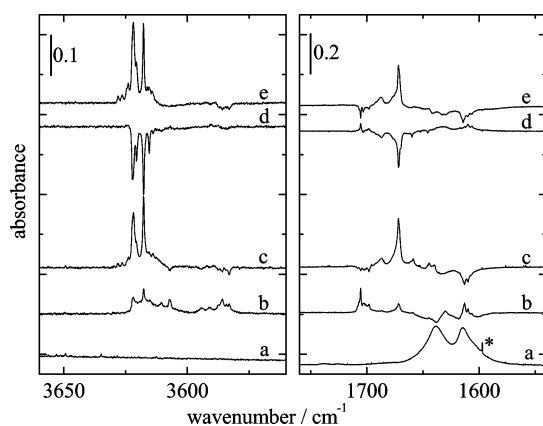
Figure 4. IR spectra of successive irradiation of acetylacetone isolated in a N_2 matrix (concentration, 1/500; temperature, 4 K): spectrum just after deposition (a), difference spectrum between after 23 min irradiation at 265 nm (mean power 8 mW) and after deposition (b), difference spectrum between 104 and 50 min irradiation at 265 nm (c), difference spectrum between 18 min irradiation at 230 nm (mean power 5 mW) and the end of irradiation at 265 nm (d), and difference spectrum between 37 min irradiation at 255 nm (mean power 6 mW) and the end of irradiation at 230 nm (e). The peak labeled with the star is due to a water impurity.

three groups: the high frequency (HF) ν_{OH} modes in the 3630–3615 cm^{-1} range, the medium frequency (MF) ν_{OH} modes in the 3615–3600 cm^{-1} range, and the low frequency (LF) ν_{OH} modes in the 3600–3575 cm^{-1} range. The $\nu_{C=O}/\nu_{C=C}$ region clearly shows the decrease of the broad peaks corresponding to the chelated form and the increase of the shifted and narrow peaks, in agreement with what is expected for non-chelated forms. In fact, the infrared spectrum for the chelated form is clearly distinct from the spectra characterizing the non-chelated forms because of the strength of the hydrogen bond, calculated[16] at 12 kcal mol^{-1}, which leads to the red-shift and the broadening of infrared lines, especially those related to the ν_{OH} mode or to the vibrational modes that strongly interact with the H-bond.

The effect of the long time irradiation at 265 nm is shown in Figure 4c. When the CCC form is almost entirely converted, there is an interconversion among the non-chelated species, namely, the bands corresponding to the LF modes decrease while the bands corresponding to the HF modes increase. It should be noted that a small band in the MF region (3607 cm^{-1}) also decreases. This indicates that the created LF isomers are now excited (the UV wavelength probably being in the wing of their absorption line) and can photoisomerize. It should be

remarked that the IR absorption cross-section is much lower for the LF isomers when compared to the HF isomers. Following this decrease of the LF isomer bands, we have performed the UV irradiation at 230 nm. Figure 4d shows that a 18 min irradiation clearly produces a considerable decrease of the HF isomer bands, whereas only a very limited decrease is observed for the LF isomer bands. We have subsequently irradiated our system at a 255 nm intermediate wavelength to excite the LF species, and we have consistently observed again the LF → HF interconversion, similar to that observed in Figure 4c, as seen in Figure 4e.

We now analyze, in considerable detail, the vibrational spectra in both the ν_{OH} and the $\nu_{C=O}/\nu_{C=C}$ regions to assign the observed bands to different isomers of acetylacetone. Clearly, this is a highly non-trivial task due to the existence of at least seven non-chelated isomers, as shown in Figure 1. The identification of the different isomers can be achieved by the analysis of the spectral correlations obtained by the irradiation-induced inter-conversions, combined with the harmonic frequency calculations, as discussed in a later part of this paper. The vibrational spectral regions considered in this work cover only a limited part of the entire infrared spectrum, but the resulting information is sufficient to distinguish between the different isomers. When irradiating CCC, three main groups of the spectral bands appear in the $\nu_{C=O}/\nu_{C=C}$ region, centered at 1703, 1672, and 1611 cm^{-1}, as seen in Figure 4b. Figure 4c shows that the two groups at 1703 and 1611 cm^{-1} are correlated with the LF and MF isomers (decreasing bands), whereas the central main band at 1672 cm^{-1} is correlated with the HF isomers (increasing bands). Table 1 also shows that the non-chelated isomers can be separated into three groups taking into account the calculated values of ν_{OH}: (i) CTC, TCC, and TTC, with low O–H stretch frequencies (3797–3809 cm^{-1}), (ii) CTT and CCT, with intermediate O–H stretch frequencies (3820–3827 cm^{-1}), and (iii) TCT and TTT, with high O–H stretch frequencies (3836–3839 cm^{-1}). They can also be separated into the alternative three groups taking into account the possible values of $\Delta\nu = |\nu_{C=O} - \nu_{C=C}|$: (i) CTC, CTT, and CCT, with large $\Delta\nu$ (81–100 cm^{-1}), (ii) TCC and TTC, with intermediate $\Delta\nu$ (27–40 cm^{-1}), and (iii) TCT and TTT, with small $\Delta\nu$ (8–9 cm^{-1}). It should be noted that the three isomers with the largest $\Delta\nu$ are also the three with the highest $\nu_{C=O}$ frequencies. Only one among these three forms, CTC, corresponds to a low frequency ν_{OH} isomer, and in consequence, the LF feature can be assigned to this isomer without ambiguity. The small band at 3607 cm^{-1} (in the MF mode region), which decreases along with the LF bands after a prolonged irradiation at 265 nm, also corresponds to a large $\Delta\nu$ value, as seen in Figure 4c. In fact, the bands at 1703 and 1611 cm^{-1} are multiplets, and experiments show, through their behavior after various irradiation periods, that at least two distinct isomers contribute to these bands. Thus, the MF isomer could be CTT or CCT, according to their $\Delta\nu$ and ν_{OH} characteristics. An additional observation of the changes in the spectrum after a night of sample irradiation, merely by the spectrometer globar source, has shown a conversion of the MF isomer to CTC. The infrared-induced interconversion can only concern the rotations around single bonds since the energy of the photon is too low to induce a rotation around a double bond. We can therefore deduce that the MF isomer is CTT and not CCT and that the globar light induces the rotation around the C–O single bond. Concerning the HF isomers, our vibrational frequency calculations show that they are probably TCT or TTT. This would be consistent with the high-intensity peak at 1672 cm^{-1} which increases or decreases in correlation with the ν_{OH}

Acetylacetone and Its Isomers

J. Phys. Chem. A, Vol. 110, No. 11, 2006 **3923**

peaks. When scaling this frequency by the ratio between the calculated and experimental mean frequencies of the high-frequency $\nu_{C=O}$ modes (CTC, CTT and CCT), i.e., $1.02 = 1741/1703$, we obtain an expected calculated value of 1705 cm^{-1}, which perfectly fits the calculated mean value for the other four isomers (TCC, TCT, TTC, and TTT). Their $\nu_{C=O}$ frequencies are nevertheless all close to this mean value and therefore they cannot be further distinguished in this way. The complete assignments of all the bands and the full identification of all the isomers is beyond the scope of this paper and will be done in a forthcoming publication, using additional experiments involving selective IR irradiations.

The results presented above show that the UV absorption spectrum of acetylacetone and its isomers isolated in a nitrogen matrix consists of broad bands (fwhm of typically 30 nm) and that the spectra of non-chelated isomers can be analyzed by focusing on two distinct bands. This enables us to identify two among the seven non-chelated isomers of acetylacetone, i.e., CTC and CTT, for which the absorption is centered at 249 nm. The UV absorption for CCC is centered at 265 nm and that of the other forms is centered at 230 nm.

III. Theory

A. Method. To understand the shifts in the UV spectra that are obtained after irradiating acetylacetone with light tuned at 265 nm, we performed highly accurate ab initio calculations of the UV transition energies and dipole oscillator strengths corresponding to a few lowest-energy singlet states of each of the eight forms of acetylacetone (optimized at the B3LYP/6-311++G(2d,2p)level of theory) shown in Figure 1. In the best calculations we could afford, we used the state-of-the-art CR-EOMCCSD(T) method.[33,35,36] This high-level method had to be employed to get a reliable description of the observed UV transitions. The CR-EOMCCSD(T) approach is based on the EOMCC extension[38,39] of the ground-state coupled-cluster theory[40-44] to excited electronic states. We also used the basic EOMCC singles and doubles (EOMCCSD) approach.[38,39] We now briefly describe the most essential details of the EOMCCSD and CR-EOMCCSD(T) calculations, relevant for this study.

In the EOMCCSD method, one represents excited electronic states $|\Psi_K\rangle$ by applying the linear excitation operator $R_K^{(CCSD)} = R_0 + R_1 + R_2$ (R_n is an n-body or n-triply excited component of $R_K^{(CCSD)}$) to the ground state $|\Psi_0\rangle = \exp(T^{(CCSD)})|\Phi\rangle$ resulting from the standard CCSD (coupled-cluster singles and doubles[45-48]) calculations. Here, we use a notation in which $T^{(CCSD)} = T_1 + T_2$ is the cluster operator obtained in the CCSD calculations, T_1 and T_2 are the one- and two-body components of $T^{(CCSD)}$, and $|\Phi\rangle$ is the reference determinant (we used the restricted Hartree-Fock (RHF) determinant as a reference in our calculations). The EOMCCSD excitation operators $R_K^{(CCSD)}$ and the corresponding vertical excitation energies $\omega_K^{(EOMCCSD)}$ are obtained by diagonalizing the similarity transformed Hamiltonian $\bar{H}^{(CCSD)} = \exp(-T^{(CCSD)}) H \exp(T^{(CCSD)})$ in a space of singly and doubly excited determinants relative to $|\Phi\rangle$.

The low-lying states of acetylacetone are dominated by one-electron transitions. The EOMCCSD approximation is known to provide reasonable results for such states (the resulting errors in excitation energies should not exceed 0.3-0.5 eV), but if we want to improve the accuracies to a $\sim$0.1 eV level and obtain a better balance between different excited states, we have to include the essential effects due to triple excitations (cf., e.g., refs 33, 35, and 36 and references therein). Ideally, one would like to use the full EOMCCSDT (equation-of-motion coupled-cluster method with singles, doubles, and triples)[49-51] to describe

triples effects, but presently the applicability of the EOMCCSDT method is limited to molecules which are much smaller than acetylacetone due to the prohibitively large costs of the EOMCCSDT calculations. The CR-EOMCCSD(T) methods used in this study describe the most important triples effects via the a posteriori non-iterative corrections to EOMCCSD energies, which are much less expensive than the EOMCCSDT calculations.

There are several variants of the CR-EOMCCSD(T) method[35] (all based on the extension of the formalism of the method of moments of coupled-cluster equations[32-34,36,52] to excited electronic states[33,36,53,54]). In this study, we used the so-called $\delta(ID)$ and $\delta(IID)$ CR-EOMCCSD(T) approximations, in which the suitably defined non-iterative corrections due to triply excited determinants are directly added to the vertical excitation energies $\omega_K^{(EOMCCSD)}$ obtained in the EOMCCSD calculations. We used these two different variants of the CR-EOMCCSD(T) theory, since the $\delta(ID)$ approximation usually provides upper bounds to the calculated excitation energies, whereas the $\delta(IID)$ excitation energies may be somewhat below the exact (meaning, full CI) values in a given basis set. The corresponding vertical excitation energies $\omega_K \equiv \omega_K(X)$, where $X = \delta(ID)$, $\delta(IID)$, are calculated as follows (cf., e.g., ref 35):

$$\omega_K = \omega_K^{(EOMCCSD)} + \sum_{i<j<k, a<b<c} \langle \tilde{\Psi}_K(X)|\Phi_{ijk}^{abc}\rangle \mathscr{M}_{abc}^{ijk}(K)/\Delta_K(X). \quad (1)$$

Here, i, j, k (a, b, c) are the occupied (unoccupied) spin-orbitals and $|\Phi_{ijk}^{abc}\rangle$ are the triply excited determinants relative to the RHF reference. The $\mathscr{M}_{abc}^{ijk}(K)$ coefficients in eq 1 represent the generalized moments of the EOMCCSD equations obtained by projecting these equations on triply excited determinants.[53,54] They can be easily calculated using the aforementioned CCSD and EOMCCSD cluster and excitation operators, $T^{(CCSD)}$ and $R_K^{(CCSD)}$, respectively. We can write

$$\mathscr{M}_{abc}^{ijk}(K) = \langle \Phi_{ijk}^{abc}| \bar{H}^{(CCSD)}R_K^{(CCSD)}|\Phi\rangle, \quad (2)$$

where $\bar{H}^{(CCSD)}$ is the similarity transformed Hamiltonian of the CCSD theory. The $\Delta_K(X)$ denominators in eq 1 are defined as

$$\Delta_K(X) = \langle \tilde{\Psi}_K(X)| R_K^{(CCSD)}\exp(T^{(CCSD)})|\Phi\rangle, \quad (3)$$

where

$$| \tilde{\Psi}_K(\delta(ID))\rangle = (P + Q_1 + Q_2 + Q_3)(R_K^{(CCSD)} + \tilde{R}_3)e^{T(CCSD)}|\Phi\rangle \quad (4)$$

and

$$| \tilde{\Psi}_K(\delta(IID))\rangle = (P + Q_1 + Q_2)R_K^{(CCSD)}e^{T(CCSD)}|\Phi\rangle + \tilde{R}_3|\Phi\rangle, \quad (5)$$

with

$$\tilde{R}_3|\Phi\rangle = \sum_{i<j<k, a<b<c} |\mathscr{M}_{abc}^{ijk}(K)/D_{ijk}^{abc}(K)]|\Phi_{ijk}^{abc}\rangle \quad (6)$$

representing the perturbative estimate of the triply excited component of the excitation operator R_K that defines excited states in the EOMCC theory. The operators P and Q_1, Q_2, and Q_3 represent the projection operators on the manifolds spanned by the reference determinant $|\Phi\rangle$ and the singly, doubly, and

TABLE 2: Ground-State Energies of the Isomers of Acetylacetone (in kcal mol^{-1}) (a) Relative to the CCC Chelated Form and (b) Relative to the CTC Nonchelated Form, As Obtained by the B3LYP/6-311++G(2d,2p) and the CR-CCSD(T)/6-31++G(d,p) Methods[a]

	(B3LYP/6-311++G(2d,2p))		(CR−CCSD(T)/6-31++G(d,p))	
isomer	part a	part b	part a	part b
CCC	0.0		0.0	
CTC	11.1	0.0	10.0	0.0
CTT	11.8	0.7	11.1	1.1
TCC	12.7	1.7	12.1	2.1
TCT	13.6	2.5	12.0	2.0
TTC	14.3	3.2	13.3	3.3
CCT	15.6	4.5	14.7	4.7
TTT	16.6	5.5	16.0	6.0

[a] Variant IID of the CR−CCSD(T) method, as defined in ref 35, has been used.

triply excited determinants, respectively. Finally, the $D_{ijk}^{abc}(K)$ denominators entering eq 6 are defined as

$$D_{ijk}^{abc}(K) = E_K^{(EOMCCSD)} - \langle \Phi_{ijk}^{abc}| \bar{H}^{(CCSD)}|\Phi_{ijk}^{abc}\rangle, \quad (7)$$

where $E_K^{(EOMCCSD)}$ is the EOMCCSD energy of state K; i.e., we use the diagonal part of the triples-triples block of matrix representing $\bar{H}^{(CCSD)}$ to calculate $D_{ijk}^{abc}(K)$.

The EOMCCSD and CR-EOMCCSD(T) calculations and the corresponding ground-state CCSD and CR-CCSD(T)[32−35] calculations were performed using the system of CC and EOMCC computer programs[35,55,56] that are the integral part of the GAMESS package.[57] To determine which of the calculated excited states represent the dipole-allowed transitions, we calculated the corresponding oscillator strengths at the EOM-CCSD level of theory, also using the EOMCC computer codes[56] that are part of GAMESS.[57] In all CC and EOMCC calculations, we used the 6-31++G(d,p) basis set,[58−60] and the lowest seven orbitals correlating with the 1s orbitals of the carbon and oxygen atoms were kept frozen. In the following, we focus on the three lowest-energy excited states for each isomer of acetylacetone discussed in this study.

B. Results. The ground-state (S$_0$) energies obtained by the standard B3LYP/6-311++G(2d,2p) and CR-CCSD(T)/6-31++G-(d,p) levels of theory (the latter using variant IID of CR-CCSD-(T)[55]) are summarized in Table 2. The chelated CCC form is most stable, by more than 10 kcal mol^{-1}, in both calculations. Among the non-chelated forms, CTC is most stable and the highest-energy TTT isomer is less stable than CTC by about 6 kcal mol^{-1}. The five most stable non-chelated forms—CTC, CTT, TCC, TCT, and TTC—lie between 10 and 14 kcal mol^{-1} above CCC, whereas the two least stable isomers, CCT and TTT, are at 5−6 kcal mol^{-1} above CTC. The instability of CCT is due to hindering between the sp^2 and sp^3 electron pairs located on each oxygen atom while that of TTC and TTT is due to steric hindering between the two methyl groups. TTC is more stable than TTT because of the long-range electrostatic interaction between the sp^3 enolic oxygen electron pair and the methyl group, as described recently by Kank Jensen et al.,[61] and this is in agreement with the increase in Mulliken's charges of the two methyl groups, from −0.058 e for TTT to −0.084 e for TTC according to our B3LYP calculations. Note that, as expected, when the methyl groups are in *syn*-1,3 interaction (TTC and TTT isomers), their relative configuration is staggered. For the other isomers, the small interactions, either attractive with the O lone pair orbitals, or repulsive with the H atom of the OH group, determine the relative configurations of the methyl

TABLE 3: Vertical Excitation Energies (in eV) Corresponding to the Three Lowest Energy Excited States of Each Isomer of Acetylacetone, Obtained with the CR-EOMCCSD(T) δ(ID) (Denoted δ(ID)) and CR-EOMCCSD(T) δ(IID) (Denoted δ(IID)) Methods[a]

	EOMCCSD	δ(ID)	δ(IID)	dipole oscillator strengths
CCC	4.565	4.396	3.994	0.5963×10^{-3}
	5.522	5.234	4.969	0.3497
	6.089	5.940	5.751	0.9272×10^{-2}
CTC	4.347	4.184	3.788	0.2691×10^{-3}
	5.787	5.636	5.449	0.3326×10^{-2}
	5.872	5.603	5.356	0.4164
CTT	4.327	4.163	3.765	0.2288×10^{-3}
	5.849	5.577	5.328	0.4170
	5.911	5.753	5.539	0.1295×10^{-4}
TCC	4.401	4.236	3.875	0.2259×10^{-3}
	6.096	5.825	5.545	0.4324
	6.132	5.968	5.774	0.3325×10^{-2}
TCT	4.335	4.168	3.801	0.2045×10^{-3}
	5.822	5.665	5.450	0.1954×10^{-4}
	6.256	6.105	5.668	0.3139
TTC	4.412	4.251	3.880	0.1571×10^{-3}
	5.963	5.806	5.624	0.2094×10^{-2}
	6.171	5.902	5.643	0.5116
CCT	4.192	4.031	3.653	0.2734×10^{-3}
	5.790	5.635	5.425	0.6097×10^{-3}
	6.049	5.808	5.543	0.4466
TTT	4.368	4.203	3.834	0.1138×10^{-3}
	5.857	5.708	5.481	0.1221×10^{-3}
	6.152	5.894	5.618	0.5013

[a] Dipole oscillator strengths were obtained with the EOMCCSD method.

groups. In the case of CCC and CCT, they are staggered, while in the cases of CTC, CTT, TCC, TCT, they are eclipsed.

Although the CR-CCSD(T)IID/6-31++G(d,p) energies are expected to be more reliable than the corresponding density functional theory data, it is interesting to note that the considerably less expensive B3LYP method gives very similar relative energies and almost the same isomer energy ordering. The only exceptions, where the CR-CCSD(T) and B3LYP energy orderings differ, are the TCC and TCT isomers. These two isomers are rather close in energy, so it is not entirely surprising that their ordering in different calculations can be different.

Table 3 shows the vertical excitation energies of the three lowest-energy excited states of acetylacetone and its non-chelated isomers, calculated by the EOMCCSD and CR-EOMCCSD(T) methods. It can be noted that the CR-EOMCCSD-(T) methods lower the EOMCCSD excitation energies for the lowest-energy dipole-allowed electronic transitions by ∼0.1−0.6 eV. This is rather typical for such calculations: the EOMCCSD excitation energies are expected to be located above the exact energy values, while the CR-EOMCCSD(T) approaches lower the EOMCCSD energies, bringing them closer to the exact excitation energies in a given basis set. Table 3 shows that the first strongly dipole-allowed transition ($\pi \rightarrow \pi^*$ excitation) occurs between S$_0$ and S$_2$ for CCC, CTT, and TCC, and between S$_0$ and S$_3$ for CTC, TCT, TTC, CCT and TTT, but not between S$_0$ and S$_1$ (n $\rightarrow \pi^*$ excitation). The numbering of the states is here relative to the vertical relative energies. A more careful analysis of the nature of excited states of acetylacetone, based on the one-electron reduced density matrices obtained with the EOMCCSD and CR-EOMCCSD-(T) approaches, may be required to provide further insights. We plan to perform such studies in the future work. We will also examine the effect of the basis set: typically, the use of larger basis sets lowers the excitation energies, making them closer to experiment, but we do not expect this effect to change

Acetylacetone and Its Isomers

J. Phys. Chem. A, Vol. 110, No. 11, 2006 **3925**

TABLE 4: Vertical Excitation Wavelengths (in nm) for the Lowest Energy Allowed Electronic Transition of the Isomers of Acetylacetone, Obtained with EOMCCSD, CR-EOMCCSD(T) δ(ID) (Denoted δ(ID)), and CR-EOMCCSD(T) δ(IID) (Denoted δ(IID)) Methods[a]

	EOMCCSD	δ(ID)	δ(IID)	dipole oscillator strengths
CCC	224	237	250	0.35
CTC	211	221	231	0.42
CTT	212	222	233	0.42
TCC	203	213	224	0.43
TCT	198	203	219	0.31
TTC	201	210	220	0.51
CCT	205	213	223	0.45
TTT	201	210	221	0.50

[a] Dipole oscillator strengths were obtained with the EOMCCSD method.

the excitation energy shifts between the chelated and the non-chelated forms significantly, since we expect a similar amount of lowering for all isomers. For the sake of clarity, the wavelengths of the dipole-allowed transitions (nonzero oscillator strength) are also gathered in Table 4. According to the CR-EOMCCSD(T) δ(IID) calculations (column c in Table 4), we can roughly divide the isomers of acetylacetone into the following three groups: (i) CCC, for which the transition wavelength is 250 nm, (ii) CTC and CTT, for which the transition wavelengths are around 230 nm (mean value 232 nm), and (iii) TCC, TCT, TTC, CCT, and TTT, for which the transition wavelengths are around 220 (mean value 221 nm).

IV. Discussion

The gas-phase value of the UV absorption wavelength for the basic enol form of acetylacetone is 266 nm and the value that we have obtained (265 nm) from the N_2 matrix isolation study is very similar. The UV absorption is not expected to be strongly modified by interactions with inert matrices, like rare gas or nitrogen matrices, and our experiment confirms this. The CR-EOMCCSD(T) methods, particularly CR-EOMCCSD(T) δ-(IID), succeed in reproducing the most essential experimental features of the UV absorption for the acetylacetone isomers. The excitation wavelength of 250 nm obtained for CCC is not too far removed from the experimental value of 265 nm. Perhaps more importantly, the blue-shift of ~29 nm obtained for the TCC, TCT, TTC, CCT, and TTT isomers fits well the experimental shift of 35 nm between the non-chelated forms, which absorb around 230 nm, and the chelated form, which absorbs around 265 nm. In addition, the theoretical evidence for the existence of two isomers of acetylacetone which absorb at the intermediate mean wavelength of 232 nm (the theoretical blue-shift relative to CCC of 18 nm) is also in complete agreement with our assignment of the intermediate UV absorption found around 249 nm to CTC and CTT (the experimental blue-shift is 16 nm).

The experimental assignment can be done here thanks to the UV excitation effects ($S_0 \rightarrow S_2$ or $S_0 \rightarrow S_3$), followed by relaxation that leads to isomerization. It should be noted though that the electronic states S_n are assigned here using the theoretical energy ordering calculated for the vertical transitions. The actual potential energy surfaces of the ground and excited states are far from being well understood, and it is possible that the UV relaxation involves curve-crossing phenomena, as shown earlier for malonaldehyde.[11]

The experimental assignment is partly based on separating the isomers into three groups according to their ν_{OH} frequencies and on comparing the resulting groups with the results of

harmonic frequency calculations. Thus, we have to be careful in drawing final conclusions, because several factors can affect our interpretation of experiment, such as (i) the limited accuracy of the vibrational frequency calculations, (ii) the proximity of the three experimental frequency domains (especially for the LF and MF domains), and (iii) the possible blurring of the frequency assignment due to site effects. In fact, it is well-known that matrix environment can induce multiple and shifted frequencies for a single vibrational mode, shifts being typically on the order of a few wavenumbers. Therefore, we have taken great care to distinguish the site effects from the isomer effects by analyzing both the temperature and irradiation effects. In addition, the consistency of our assignments is based on the correlations between different spectral domains and changes in the infrared absorption observed after UV irradiation, which we observed in a large number of experiments.

The two non-chelated forms (CTC and CTT) absorbing at a red-shifted UV wavelength compared to the other non-chelated isomers differ only by a rotation around the single C—O bond, and the C=O and C=C bonds are in a cis configuration in both isomers. This would suggest the existence of a larger degree of conjugation in the CTC and CTT isomers compared to other non-chelated forms, explaining the observed shift of the UV transition relative to CCC, which is smaller compared to other non-chelated forms, as well as the large values of the $\Delta\nu$ and ν_{CO} frequency values. Calculations show that the CCT, CTC, and CTT isomers have very similar infrared characteristics in the ν_{CO}/ν_{CC} domain, in agreement with an equally high level of conjugation in these three isomers. On the other hand, our calculations show that the CCT isomer is much higher in energy compared to the CTC and CTT forms. This can be explored by the repulsive interaction between the sp^2 and sp^3 groups of the two oxygen atoms.

V. Conclusions

The primary objective of this study was to calculate the UV transition energies of the different isomers of acetylacetone and to compare them to the experimental results. The cryogenic matrix isolation allowed us to create and observe the high-energy non-chelated isomers of acetylacetone by exciting its $\pi \rightarrow \pi*$ transition at 265 nm. We subsequently used the UV spectroscopy to determine the photoabsorption spectra of various isomers of acetylacetone and we also reversely excited the $\pi \rightarrow \pi*$ transitions of the non-chelated forms produced after the initial UV irradiation. All of these UV excitations, combined with the standard B3LYP frequency calculations and FTIR spectroscopy, allowed us to provide a strong evidence for the identification of the non-chelated isomers of acetylacetone which can be obtained by irradiating the chelated CCC isomer with the UV light. To support our experimental findings, the ground and excited states of various forms of acetylacetone were examined with the high-level ab initio methods based on the EOMCC theory. The most accurate CR-EOMCCSD(T) calculations confirmed the assignment of the $S_0 \rightarrow S_1$ dipole forbidden transition to the transition to a $n\pi*$ state while S_2 or S_3 correspond to the $\pi\pi*$ state involved in the dipole-allowed transition of both chelated and non-chelated forms. The transition energy values obtained with the CR-EOMCCSD(T) method are in very good agreement with those found experimentally. Because of the loss of conjugation, there is a large blue-shift in the UV photoabsorption characterizing the non-chelated isomers and the CR-EOMCCSD(T) calculations confirm this. The experimental and CR-EOMCCSD(T) values of this shift are 35 and 29 nm, respectively, if we focus on the TCC, TCT, TTC,

CCT, and TTT isomers, and 16 and 18 nm, respectively, if we focus on the CTC and CTT isomers. The theoretical and experimental results also agree with regard to the identification of two non-chelated isomers of acetylacetone (CTC and CTT), which absorb to the red compared to the remaining five non-chelated isomers.

References and Notes

(1) Chiavassa, T.; Roubin, P.; Pizzala, L.; Verlaque, P.; Allouche, A.; Marinelli, F. *J. Phys. Chem.* **1992**, *96*, 10659.

(2) Chiavassa, T.; Verlaque, P.; Pizzala, L.; Allouche, A.; Roubin, P. *J. Phys. Chem.* **1993**, *97*, 5917.

(3) Bauer, S. H.; Wilcox, C. F. *Chem. Phys. Lett.* **1997**, *279*, 122.

(4) Chong, D. P.; Hu, C.-H. *J. Electron Spectrosc. Relat. Phenom.* **1998**, *94*, 181.

(5) Sobolewski, A. L.; Domcke, W. *J. Phys. Chem. A* **1999**, *103*, 4494.

(6) Sobolewski, A. L.; Domcke, W. *Chem. Phys. Lett.* **1999**, *300*, 533.

(7) Alparone, A.; Millefiori, S. *Chem. Phys.* **2002**, *290*, 15.

(8) Meyer, R.; Ha, T. K. *Mol. Phys.* **2003**, *101*, 3263.

(9) Hayashi, T.; Mukamel, S. *J. Phys. Chem. A* **2003**, *107*, 9113.

(10) Kovacevic, G.; Hrenar, T.; Doslic, N. *Chem. Phys.* **2003**, *293*, 41.

(11) Coe, J. D.; Martinez, T. J. *J. Am. Chem. Soc.* **2005**, *127*, 4560.

(12) Iijima, K.; Ohnogi, A.; Shibata, S. *J. Mol. Struct.* **1987**, *156*, 111.

(13) Rios, M. A.; Rodríguez, J. *J. Mol. Struct. (THEOCHEM)* **1990**, *204*, 63.

(14) Roubin, P.; Chiavassa, T.; Verlaque, P.; Pizzala, L.; Bodot, H. *Chem. Phys. Lett.* **1990**, *175*, 655.

(15) Chiavassa, T.; Verlaque, P.; Pizzala, L.; Roubin, P. *Spectrochim. Acta, Part A* **1994**, *50*, 343.

(16) Dannenberg, J. J.; Rios, R. *J. Phys. Chem.* **1994**, *98*, 6714.

(17) Hinsen, K.; Roux, B. *J. Chem. Phys.* **1997**, *106*, 3567.

(18) Boese, R.; Antipin, M. Y.; Bläser, D.; Lyssenko, K. A. *J. Phys. Chem. B* **1998**, *102*, 8654.

(19) Ishida, T.; Hirata, F.; Kato, S. *J. Chem. Phys.* **1999**, *110*, 3938.

(20) Yoon, M.-C.; Choi, Y. S.; Kim, S. K. *J. Chem. Phys.* **1999**, *110*, 11850.

(21) Yoon, M.-C.; Choi, Y. S.; Kim, S. K. *Chem. Phys. Lett.* **1999**, *300*, 207.

(22) Tayyari, S. F.; Milani-Nejad, F. *Spectrochim. Acta, Part A* **2000**, *56*, 2679.

(23) Nagashima, N.; Kudoh, S.; Takayanagi, M.; Nakata, M. *J. Phys. Chem. A* **2001**, *105*, 10832.

(24) Mavri, J.; Grdadolnik, J. *J. Phys. Chem. A* **2001**, *105*, 2039.

(25) Mavri, J.; Grdadolnik, J. *J. Phys. Chem. A* **2001**, *105*, 2045.

(26) Upadhyaya, H. P.; Kumar, A.; Naik, P. D. *J. Chem. Phys.* **2003**, *118*, 2590.

(27) Coussan, S.; Manca, C.; Ferro, Y.; Roubin, P. *Chem. Phys. Lett.* **2003**, *370*, 118.

(28) Srinivasan, R.; Feenstra, J. S.; Park, S. T.; Xu, S.; Zewail, A. H. *J. Am. Chem. Soc.* **2004**, *126*, 2266.

(29) Xu, S.; Park, S. T.; Feenstra, J. S.; Srinivasan, R.; Zewail, A. H. *J. Phys. Chem. A* **2004**, *108*, 6650.

(30) Matanivić, I.; Došlić, N. *J. Phys. Chem. A* **2005**, *109*, 4185.

(31) Temprado, M.; Roux, M. V.; Umnahanant, P.; Zhao, H.; Chickos, J. S. *J. Phys. Chem. B* **2005**, *109*, 12590.

(32) Kowalski, K.; Piecuch, P. *J. Chem. Phys.* **2000**, *113*, 18.

(33) Piecuch, P.; Kowalski, K.; Pimienta, I. S. O.; McGuire, M. J. *Int. Rev. Phys. Chem.* **2002**, *21*, 527.

(34) Piecuch, P.; Kowalski, K.; Fan, P.-D.; Pimienta, I. S. O. In *Advanced Topics in Theoretical Chemical Physics*; Maruani, J., Lefebvre, R., Brändas, E., Eds.; Progress in Theoretical Chemistry and Physics 12; Kluwer: Dordrecht, The Netherlands 2003; pp 119−206.

(35) Piecuch, P.; Kowalski, K. *J. Chem. Phys.* **2004**, *120*, 1715.

(36) Piecuch, P.; Kowalski, K.; Pimienta, I. S. O.; Fan, P.-D.; Lodriguito, M.; McGuire, M. J.; Kucharski, S. A.; Kuś, T.; Musiał, M. *Theor. Chem. Acc.* **2004**, *112*, 249.

(37) Frisch, M. J.; et al. Gaussian98, Rev. A.2. Gaussian Inc.: Pittsburgh, PA, 1998.

(38) Geertsen, J.; Rittby, M.; Bartlett, R. J. *Chem. Phys. Lett.* **1989**, *164*, 57.

(39) Stanton, J. F.; Bartlett, R. J. *J. Chem. Phys.* **1993**, *98*, 7029.

(40) Coester, F. *Nucl. Phys.* **1958**, *7*, 421.

(41) Coester, F.; Kümmel, H. *Nucl. Phys.* **1960**, *17*, 477.

(42) Čížek, J. *J. Chem. Phys.* **1966**, *45*, 4256.

(43) Čížek, J. *Adv. Chem. Phys.* **1969**, *14*, 35.

(44) Čížek, J.; Paldus, J. *Int. J. Quantum Chem.* **1971**, *5*, 359.

(45) Purvis, G. D., III; Bartlett, R. J. *J. Chem. Phys.* **1982**, *76*, 1910.

(46) Scuseria, G. E.; Scheiner, A. C.; Lee, T. J.; Rice, J. E.; Schaefer, H. F., III. *J. Chem. Phys.* **1987**, *86*, 2881.

(47) Lee, T. J.; Rice, J. E. *Chem. Phys. Lett.* **1988**, *150*, 406.

(48) Piecuch, P.; Paldus, J. *Int. J. Quantum Chem.* **1989**, *36*, 429.

(49) Kowalski, K.; Piecuch, P. *J. Chem. Phys.* **2001**, *115*, 643.

(50) Kowalski, K.; Piecuch, P. *Chem. Phys. Lett.* **2001**, *347*, 237.

(51) Kucharski, S. A.; Włoch, M.; Musiał, M.; Bartlett, R. J. *J. Chem. Phys.* **2001**, *115*, 8263.

(52) Kowalski, K.; Piecuch, P. *Computational Chemistry: Reviews of Currents Trends*; Leszczyński, J., World Scientific: Singapore, 2000; Vol. 5, pp 1−104.

(53) Kowalski, K.; Piecuch, P. *J. Chem. Phys.* **2001**, *115*, 2966.

(54) Kowalski, K.; Piecuch, P. *J. Chem. Phys.* **2002**, *116*, 7411.

(55) Piecuch, P.; Kucharski, S. A.; Kowalski, K.; Musiał, M. *Comput. Phys. Commun.* **2002**, *149*, 71.

(56) Włoch, M.; Gour, J. R.; Kowalski, K.; Piecuch, P. *J. Chem. Phys.* **2005**, *122*, 214107.

(57) Schmidt, M. W.; Baldridge, K. K.; Boatz, J. A.; Elbert, S. T.; Gordon, M. S.; Jensen, J. H.; Koseki, S.; Matsunaga, N.; Nguyen, K. A.; Su, S. J.; Windus, T. L.; Dupuis, M.; Montgomery, J. A. *J. Comput. Chem.* **1993**, *14*, 1347.

(58) Clark, T.; Chandrasekhar, J.; Spitznagel, G. W.; von, R. Schleyer, P. *J. Comput. Chem.* **1983**, *4*, 294.

(59) Hehre, W. J.; Ditchfield, R.; Pople, J. A. *J. Chem. Phys.* **1972**, *56*, 2257.

(60) Hariharan, P. C.; Pople, J. A. *Theor. Chim. Acta* **1973**, *28*, 213.

(61) Jensen, S. J. K.; Tang, T.-H.; Csizmadia, I. G. *J. Phys. Chem. A* **2003**, *107*, 8975.